



HAL
open science

The conformational landscape of myrtenol: the structure of the hydroxymethyl group and its robustness upon hydration

Elias M. Neeman, N Osseiran, Thérèse Huet

► **To cite this version:**

Elias M. Neeman, N Osseiran, Thérèse Huet. The conformational landscape of myrtenol: the structure of the hydroxymethyl group and its robustness upon hydration. *The Journal of Chemical Physics*, 2022, 156 (12), pp.124301. 10.1063/5.0084562 . hal-03635175

HAL Id: hal-03635175

<https://hal.science/hal-03635175v1>

Submitted on 8 Apr 2022

HAL is a multi-disciplinary open access archive for the deposit and dissemination of scientific research documents, whether they are published or not. The documents may come from teaching and research institutions in France or abroad, or from public or private research centers.

L'archive ouverte pluridisciplinaire **HAL**, est destinée au dépôt et à la diffusion de documents scientifiques de niveau recherche, publiés ou non, émanant des établissements d'enseignement et de recherche français ou étrangers, des laboratoires publics ou privés.

The conformational landscape of myrtenol: the structure of the hydroxymethyl group and its robustness upon hydration

E. M. Neeman^{*a}, N. Osseiran^a and T. R. Huet^a

^a Univ. Lille, CNRS, UMR 8523 - PhLAM - Physique des Lasers Atomes et Molécules, F-59000 Lille, France.

* Corresponding author: Elias.neeman@univ-lille.fr

Abstract

The conformational landscape of myrtenol (2-Pinen-10-ol) and its robustness upon hydration was investigated theoretically and experimentally employing a synergic combination of quantum chemical calculations and Fourier transform microwave spectroscopy coupled to a supersonic jet expansion. Relaxed potential energy surfaces have been carried out and the lowest energy conformers of the monomer were found associated with different geometry of the hydroxymethyl group than those previously reported (G. Sedo et al, *J. Mol. Spectrosc.* 356 (2019) 32). Geometry optimizations and harmonic vibrational frequency calculations allowed to characterize the equilibrium structure of the possible conformers of myrtenol. Among the nine predicted structures, four have been observed, analyzed, and identified. The controversy on the geometry was solved with the deuteration of the hydroxyl group (OD), which led to the determination of **substitution** (r_s) geometry, in agreement with the present theoretical

results. Interestingly, the four observed conformers exhibit the same orientation of OH as in the allyl alcohol molecule. Furthermore, hydrogen bonding linking myrtenol to water was studied. One monohydrate has been observed and identified. Non-covalent interactions (NCI) and NBO analysis were performed to depict the interactions responsible for the stabilization of the observed structure. We conclude that the structure of the hydroxymethyl group is robust and does not change upon hydration.

Introduction

Biogenic volatile organic compounds (BVOCs) are emitted in large quantities into the Earth's atmosphere and play a major role in atmospheric chemistry. BVOCs are known to contribute significantly to the formation of secondary organic aerosols (SOAs) and tropospheric ozone by participating in the reaction with OH radicals in the daytime and with NO₃ in the night-time.^{1,2} Besides methane and isoprene, unsaturated hydrocarbons named monoterpenes (C₁₀H₁₆) that consist of two units of isoprene are emitted from biogenic sources, mainly by a variety of plants, coniferous forests, and are considered as atmospheric pollutants. Monoterpenes represent about 11% of the total BVOCs emission,^{3,4} BVOCs are considered as precursors of SOAs.⁵ The SOAs formation mechanisms, and evolution remain poorly understood and deserve more attention,⁶ and represent a source of uncertainty for climate simulations. Aerosols play a key role in many environmental processes in which they affect the Earth's radiation balance by scattering the solar radiation and by acting as cloud condensation nuclei. They also participate in heterogeneous chemical reactions in the atmosphere and causes a considerable impact on human health because they endanger the blood and the cardiovascular system.⁷ 2-Pinen-10-ol is

also named myrtenol (6,6-Dimethylbicyclo[3.1.1]hept-2-ene-2-methanol, C₁₀H₁₆O) is one of these monoterpene alcohol emitted in the troposphere. It has a similar bicycle structure as α - and β -pinene^{8,9} and a functional hydroxymethyl group (-CH₂-OH). The atmospheric photo-oxidation of pinenes (both α - and β -pinene) produces myrtenol in the aerosol phase.^{10,11} It has been also identified in the volatile emission of *Citrus paradisi* L¹² and represents the main volatile species emitted from **the** *Taxus baccata* plant.¹³

High-resolution rotational spectroscopy is a powerful technique to study molecular structure thanks to its sensitivity to small changes. Previous studies have shown that the synergic combination of experimental **measurements** and theoretical calculations is decisive to identify the observed conformers.^{14–17} For example, the orientation of the hydroxyl group (OH) was found to be crucial in the determination of the conformational map of fenchol and its complex with water.^{14,15} To our knowledge, the only structural study of myrtenol **is** the spectroscopic work of Sedo and co-workers.¹⁸ They observed the spectrum of three conformers using chirped-pulse (CP) Fourier transform microwave (FTMW) spectroscopy. They fitted the molecular parameters unambiguously and proposed three structures associated with different geometries of the hydroxymethyl functional group. **For all conformers, the proposed structures possess the same orientation of the OH group, differing only by the orientation of the -CH₂OH group.** Interestingly, this position of the hydroxyl group with respect to the methylene group differs substantially from the observed conformers of the allyl alcohol.^{19,20}

In the present study, we report on the conformational map of myrtenol and its complex with water, studied by impulse Fabry–Pérot Fourier transform microwave spectroscopy technique coupled to a pulsed molecular jet expansion.^{8,21} Chemically, myrtenol is a flexible molecule with

two possible torsional angles as shown in Figure 1. Therefore, its conformational landscape could be very rich with a large number of structural possibilities. Quantum chemical calculations were performed to identify the possible stable conformers, by considering both rotatable angles of the hydroxymethyl group. Nine different conformers have been identified by theoretical calculations. To go one step further and to identify unambiguously the observed experimental structures, we also studied the rotational spectrum of the deuterated hydroxyl (OD) functional group of myrtenol. The rotational constants of the observed isotopologues have been used to determine the substitution geometry (r_s) of the hydroxyl group.²² Herein, the conformational landscape of myrtenol has been entirely decrypted. The four observed spectra presented in the present study are associated with the lowest energy conformers. Their structure differs notably from those presented in the previous study of Sedo *et al.*¹⁸

The formation of SOA is not well understood at the molecular level. Water vapor is abundant species in the atmosphere and influences the evolution and properties of SOAs. Despite its ubiquity, the nucleation of water vapor is still poorly understood.²³ The formation of SOAs from BVOCs is enhanced in the presence of water.^{24–26} Hydrogen bonding is one of the main responsible for the formation of atmospherically relevant species and aerosol formation. Its first step of formation starts with the pre-nucleation cluster formation process by a molecular complex which forms a “critical nucleus” and grows than to a detectable size.^{27,28} In the present work, the hydration of myrtenol was also addressed, especially to understand how the water will be complex with myrtenol. Is water going to induce an alteration in the OH arrangement as in the case of fenchol?¹⁵ We observed the spectrum of one monohydrated conformer, which was

unambiguously assigned to the lowest energy conformer. The robustness of the most stable structure of myrtenol upon hydration is also discussed.

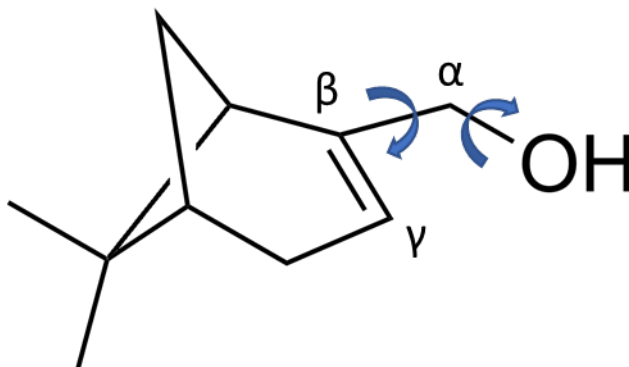


Figure 1. Chemical structure of myrtenol (6,6-Dimethylbicyclo[3.1.1]hept-2-ene-2-methanol), the torsional flexibility of the hydroxymethyl group ($C_{\gamma}=C_{\beta}-C_{\alpha}-O$ and $C_{\beta}-C_{\alpha}-O-H$) is indicated in blue arrows.

Methods

Theoretical calculations

Theoretical calculations are necessary to predict molecular properties, to help the analysis of the rotational spectra, and to facilitate the identification of the observed conformers. Only low energy conformers can survive in the adiabatic supersonic expansion and therefore their rotational spectra can be observed. Myrtenol has two flexible angles associated with the hydroxymethyl group, as marked in Figure 1. GAUSSIAN16 software package²⁹ was used to explore the potential energy surface to find its possible minima. Calculations using DFT and *ab initio* methods were performed to examine the most stable conformers of myrtenol. The

optimizations were carried out using the *ab initio* second-order perturbation theory Møller-Plesset (MP2)³⁰ and the DFT B3LYP^{31,32} methods with the Pople split-valence triple-zeta basis set augmented with diffuse and polarization functions on all atoms (the 6-311++G(d,p) basis set).³³ To predict the possible conformers of the myrtenol-water complex, all the conformers have been considered to form a hydrogen bond. For that purpose, *ab initio* calculations at MP2/6-311++G(d,p) have been performed since it gives good results for hydrates.¹⁵ The rotational constants and the electric dipole moment components are necessary for the analysis. An NBOs³⁴ analysis of the intermolecular charge transfer responsible for the relative stability of the observed myrtenol...water complex was also performed using MP2/6-311++G(d,p). Non-covalent Interaction (NCI)³⁵ analysis was also carried out using Multiwfn software³⁶ using the MP2/6-311++G(d,p) level output to plot the map of the interactions involved in the stabilization of the observed hydrated conformer.

Experimental

The pure rotation spectra of myrtenol and its water complex have been recorded in the 2–20 GHz frequency range using two impulses Fabry–Pérot supersonic jet Fourier transform microwave (FTMW) spectrometers available at the PhLAM Laboratory in Lille. The experimental setups are described in detail elsewhere.^{8,21,37} Myrtenol sample (95%) purchased from Sigma Aldrich, was used and placed into a heated nozzle at 380 K and mixed with neon as carrier gas at a backing pressure of about 4 bars. To study the hydrated myrtenol, liquid water (H₂O/D₂O) was vaporized in a reservoir placed before the sample. Then the mixture was introduced into the Fabry-Pérot cavity along the optical axis, through a 1 mm diameter pinhole using a pulsed nozzle at a

repetition rate of 1.5 Hz. The rotational temperature of the molecules in the supersonic jet is about a few Kelvin. Microwave power pulses of 2 μ s duration were used to polarize the molecules. The Free-Induction Decay (FID) signal was detected and digitized at a repetition rate of 120 MHz on a 14-bit resolution electronic card. Between 50 and 1000 FID signals were accumulated in the high-resolution measurement mode in order to obtain a good S/N ratio. After a fast Fourier transformation of the time domain signals, lines were observed as Doppler doublets. The central frequency of each line was determined by averaging the frequencies of the two Doppler components. The spectral resolution depends on the number of recorded data points, i. e. most of the time a frequency grid of 1.84 kHz using 65 536 data points, and of 3.68 kHz using 32 768 data points was applied. This grid represents the frequency difference between two recorded data points (i.e., 1 point each 1.84 or 3.68 kHz). The initial survey of the rotational spectra is performed at the low-resolution mode, using a frequency grid of 14.7 kHz, a frequency step of 250 kHz, and a repetition rate of 2 Hz.

Results and discussion

Theoretical structures and spectroscopic parameters of myrtenol

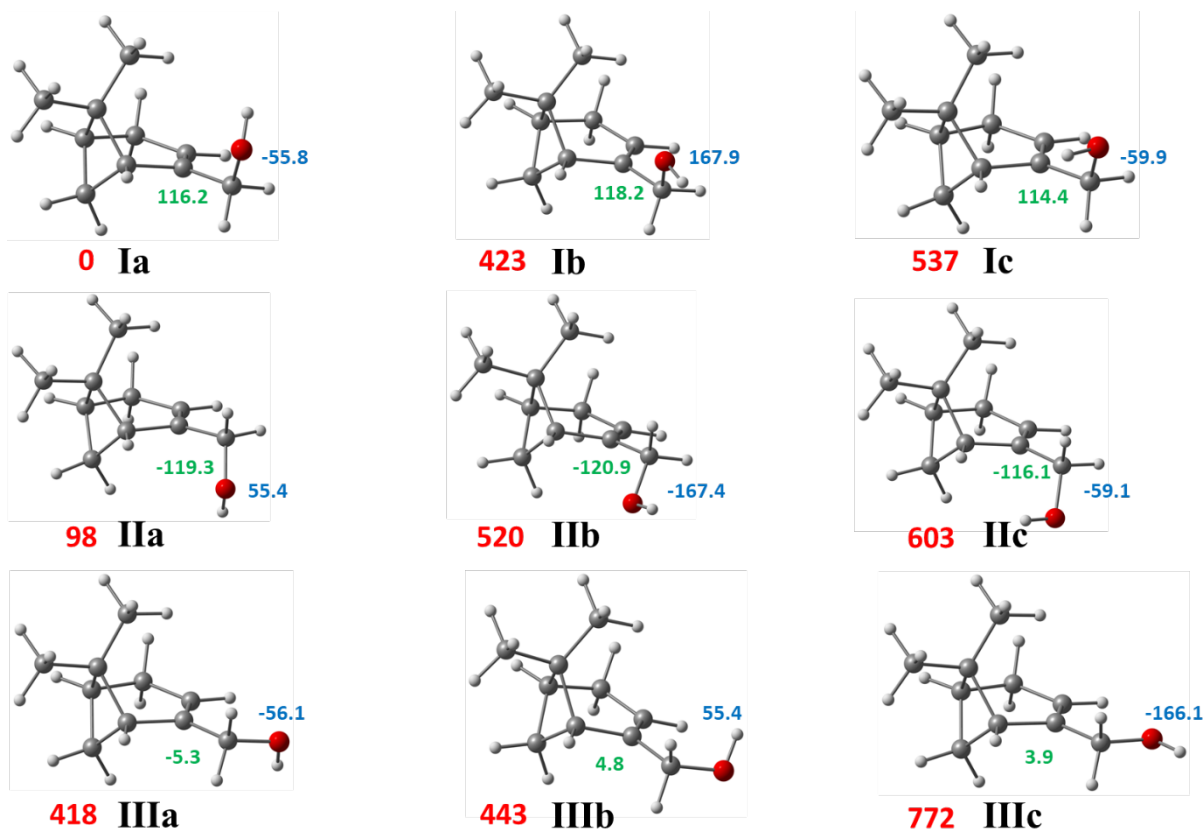


Figure 2. Visualization of the nine possible conformers of myrtenol. Their relative energies in cm^{-1} calculated at the MP2/6-311++G(d,p) level are shown in red. Roman numbers I, II, III refer to the positions of the methylene groups, and letters a, b, c indicate the increasing energy ordering. Dihedral angle ($^{\circ}$) values of $\text{C}_{\gamma}=\text{C}_{\beta}-\text{C}_{\alpha}-\text{O}$ and $\text{C}_{\beta}-\text{C}_{\alpha}-\text{O}-\text{H}$ are also indicated in green and blue, respectively.

Figure 2 shows the nine possible structures of myrtenol monomer which have been calculated. Three families of conformers have been obtained. They are associated with the three positions of the methylene bridge ($-\text{CH}_2-$) which are labeled as Roman numbers I, II, and III. Then each position the hydroxyl group (OH) is labeled as a, b and c respecting the increase of energy.

Table I. Rotational constants, relative energies, and dipole moment components of the equilibrium structure of myrtenol conformers calculated at the MP2 /6-311++G(d,p) level of theory.

Para. ^a	Ia	IIa	IIIa	Ib	IIb	IIIb	Ic	IIc	IIIc
<i>A</i>	1597.3	1711.8	1893.7	1594.9	1703.7	1870.8	1598.4	1712.6	1882.8
<i>B</i>	970.9	871.3	812.2	979.0	879.5	817.5	965.1	868.4	820.4
<i>C</i>	829.5	803.3	762.2	832.0	807.0	767.8	823.8	799.8	769.9
$ \mu_a $	1.2	1.2	1.5	0.9	0.2	1.9	1.7	2.2	0.1
$ \mu_b $	1.3	1.6	0.7	0.6	0.2	0.3	0.5	0.2	1.1
$ \mu_c $	0.8	0.0	1.0	0.9	1.4	0.6	1.0	0.4	1.1
ΔE^b	0	97.9	417.9	422.9	519.5	442.7	537.0	603.3	771.7
Δ_{ZPE}^c	0	74.2	382.3	325.0	417.2	401.9	448.4	517.5	602.2
ΔG_{380}^d	0	37.5	383.0	241.4	338.9	400.5	369.4	440.9	479.6

^a *A*, *B*, and *C* are the rotational constants given in MHz; absolute values of μ_a , μ_b , and μ_c represent the electric dipole moment components in D (1 D \approx 3.3356 \times 10⁻³⁰ C m). ^b ΔE are the relative electronic energies in cm⁻¹ with respect to the global minima calculated using the MP2 method with 6-311++G(d,p) basis set. ^c Δ_{ZPE} relative energies in cm⁻¹ including the zero-point energy correction. ^d Gibbs free energies calculated at 353 K.

The sets of spectroscopic parameters of interest of the nine calculated structures are presented in Table I. In the previous published study,¹⁸ only the three conformers Ib, IIb, and IIIc which correspond respectively to comp1, comp2, and comp3, were calculated. Meanwhile, those are not the lowest energy conformers, as could be deduced from our results presented in Table 1. In

addition, our theoretical work suggests that other lowest energy conformers could survive during the adiabatic expansion such as Ia, IIa, IIIa, and IIIb. This point will be further discussed in detail after the presentation of the observed spectra and fitted transitions.

It should be noted that the calculated quartic centrifugal parameters for the observed conformers of myrtenol are summarized in the supplementary material (Table S1), and their values compared to the experimental ones.

Observed spectra and fitted molecular parameters of myrtenol

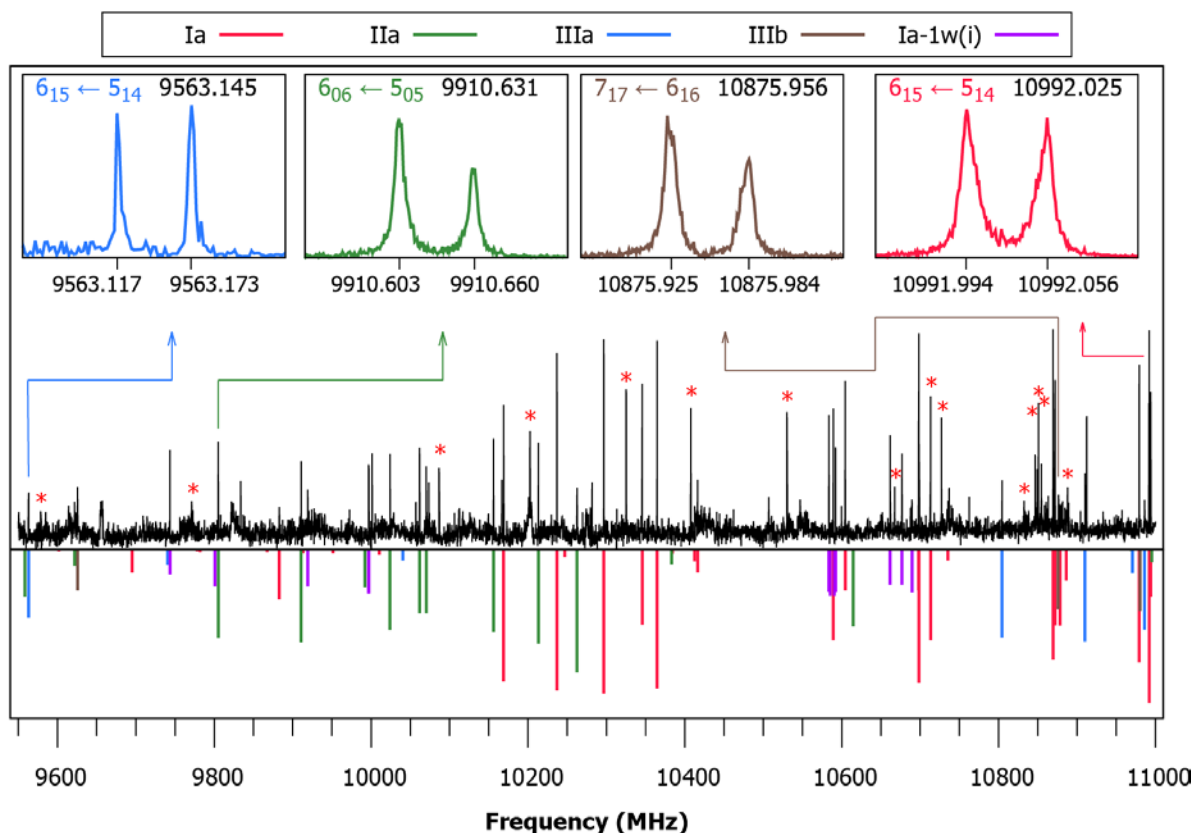


Figure 3. A portion of the low-resolution experimental spectrum shows the observed (upper part) and the simulated (lower part, $T_{\text{rot}} = 3\text{K}$) rotational lines of all the conformers of myrtenol. Intensity is in

arbitrary units. The inset shows observed rotational transitions of all the observed conformers in the high-resolution mode. The assignment of each rotational line $J_{K_a K_c} \leftarrow J'_{K'_a K'_c}$ is also indicated. Each rotational transition appears as a doublet due to the Doppler effect, because the molecular beam is parallel to the microwave radiation. The lines with an asterisk marker belong to the myrtenal molecule.

Figure 3 shows a portion of the recorded experimental spectra of myrtenol. Several lines from the three species previously observed by Sedo *et al.* have been easily identified in our spectra. They were recorded at high resolution at about $T_{\text{rot}} \approx 3$ K.¹⁵ This set of lines was merged with a secure subset of the previous data¹⁸ that could be reproduced at $T_{\text{rot}} = 15$ K, and fitted to a Watson's Hamiltonian³⁸ in the S -reduction and I' representation:

$$H_{\text{rot}}^{(S)} = B_x^{(S)} J_x^2 + B_y^{(S)} J_y^2 + B_z^{(S)} J_z^2 - D_J \vec{J}^4 - D_{JK} \vec{J}^2 J_z^2 - D_K J_z^4 + d_1 \vec{J}^2 (J_+^2 + J_-^2) + d_2 (J_+^4 + J_-^4)$$

The molecular parameters have been obtained from the analysis using the SPFIT/SPCAT suite of programs developed by Pickett.³⁹ The fitted molecular parameters are reported in Table II, their uncertainties were recalculated using the PIFORM code.⁴⁰ For the conformer Ia (Exp1 in Ref. 18), the fit includes 286 a-type, b-type, and c-type transitions (128 from this study and 158 on 314 from Ref. 18). For the conformer IIa (Exp2 in ref. 18), 209 a-type and b-type transitions (108 from this study and 101 on 118 from ref. 18) were fitted. Finally, for the conformer IIIa (Exp3 in ref. 18), the fit includes 111 a-type, b-type, and c-type transitions (70 from this study and 41 on 196 from ref. 18). For the shake of clarity, we did not consider in the fits several isolated transitions, i. e. not included in a series of lines. The same set of rotational constants as in the previous study is used. It reproduces the data at their experimental accuracy. In the end, the values of molecular parameters presented in Table II are in excellent agreement with those of Sedo *et al.*¹⁸

Table II. Rotational constants and quartic centrifugal distortion parameters of myrtenol conformers determined experimentally from the ground state.				
Par. ^a	Ia ^e	IIa ^e	IIIa ^e	IIIb
<i>A</i>	1589.311913(60)	1701.56525(10)	1887.56253(46)	1866.773(17)
<i>B</i>	971.923261(32)	871.650262(41)	810.628701(84)	815.94582(17)
<i>C</i>	827.719611(39)	802.160097(44)	760.704296(96)	765.79801(17)
<i>D_J</i>	0.09336(21)	0.04811(22)	0.02872(40)	0.03374(84)
<i>D_{JK}</i>	-0.11217(64)	-0.00462(47)	0.0941(37)	-
<i>D_K</i>	0.1428(26)	0.2453(36)	0.188(40)	-
<i>d₁</i>	-0.024323(35)	-0.010109(31)	-0.005028(84)	-
<i>d₂</i>	0.000414(26)	0.000229(16)	-	-
<i>N^b</i>	286	209	110	38
σ^c	7.9	7.4	7.6	3.5
	Ia-OD	IIa-OD	IIIa-OD	IIIb-OD
<i>A</i>	1577.27376(35)	1695.22349(21)	1885.91640(61)	1857.778(22)
<i>B</i>	958.63748(10)	854.702219(93)	794.06414(26)	800.77164(26)
<i>C</i>	817.262616(79)	789.048096(61)	745.97139(22)	753.60986(24)
<i>D_J</i>	0.09584(45)	0.04629(35)	0.02726(61)	0.0351(15)
<i>D_{JK}</i>	-0.1262(30)	[-0.00462] ^d	0.087(11)	-
<i>D_K</i>	0.144(16)	0.1088(81)	[0.188]	-
<i>d₁</i>	-0.02249(27)	-0.00813(21)	-0.00490(63)	-
<i>d₂</i>	[0.000414] ^d	[0.000229] ^d	-	
<i>N^b</i>	110	69	31	20
σ^c	2.7	2.2	2.4	3.1

^a *A*, *B*, and *C* are the rotational constants given in MHz, *D_J*, *D_{JK}*, *D_K*, *d₁*, and *d₂* are the quartic centrifugal distortion constant in kHz. ^b Number of fitted lines. ^c σ is the RMS deviation of the fit in kHz. ^d Constant values were kept fixed to the parent species. ^e Global fit of the transitions recorded in this study with a subset of those reported in ref. ¹⁸

Once the transitions of the three previously known species were assigned, a remaining set of 38 unassigned lines could be identified. These lines, being all a-type transitions, were fitted together successfully and a new set of experimental parameters was derived, leading to the identification of a new species. The spectroscopic parameters are also presented in Table II.

To consolidate the attribution of the observed conformers as Ia, IIa, IIIa, and IIIb, the spectra of the deuterated hydroxyl group (OD) species were recorded to determine the position of the hydrogen atoms of the hydroxyl group for each conformer. For that purpose, deuterated water (D_2O) was used which allows the direct proton exchange with the hydroxyl functional group of myrtenol. The molecular parameters were calculated from the obtained equilibrium structures at the MP2/6-311++G(d,p) level of theory and then scaled by a correction factor, derived from calculating the difference between the calculated and fitted rotational constants of the assigned parent species, and applying this factor to the calculated constants of the deuterated species. This process allows for a fast observation of the deuterated hydroxyl species. The efficient scaling of the rotational constants of the deuterated species can be an indication of the correct assignment of the parent species. The signature of the nuclear quadrupole interaction effect for the deuterium nucleus was very small and not well resolved, so the analysis of the deuterated species was done without using nuclear quadrupole interaction term, by using the center of frequency of the measured transitions. The fitted values of the constants at the experimental accuracy are reported in Table II. In total, 110, 69, 31 and 20 transitions have been recorded for Ia, IIa, IIIa, and IIIb, respectively. All the recorded transitions for each species are reported in the supplementary materials.

Conformational identification and molecular structure

Two different tools are used for spectral analysis: rotational constants, and electric dipole moment components. A first identification of the observed conformers is made by a comparison between the observed and the calculated molecular parameters. However, very similar values of the calculated A , B , C constants between the conformers are observed within the same family of conformers due to the small change of the moment of inertia induced by the change of the hydrogen orientation in OH. Therefore, a preliminary attribution of the observed species but not a decisive one is done. Only the two conformers Ia and IIa are attributed directly thanks to their lowest calculated energies. Another criterion to be used to attribute the conformers is the values of the electric dipole moment components. For example, the optimized values of the electric fields used in our experiments to polarize the molecules give an idea about the magnitude of each dipole moment component of the observed conformers. Indeed, it is increased or decreased for each type of line, to compensate the lower or higher value of the permanent dipole moment components, respectively. The observed transition types and the relation between them are in good agreement with the calculated dipole moments for conformers Ia ($\mu_a \approx \mu_b > \mu_c$), IIa ($\mu_b > \mu_a$), IIIa ($\mu_a > \mu_b > \mu_c$), and for the conformer IIIb only a-type lines have been observed. Consequently, the first attribution of the observed conformers is made as Ia, IIa, IIIa, and IIIb. It is worth mentioning that the absence of c-type transitions in the case of conformer IIa can further support the new assignment in this work. The conformer IIa has its dipole moment along the c-axis equals to zero, whereas the IIb (comp2 as reported in ref. 18) conformer has its strongest component along the c-axis, and should exhibit c-type transitions.

The two sets of experimental rotational constants of the parent OH and deuterated OD isotopologues have been obtained experimentally for each observed conformer of myrtenol. Those experimental sets are used together to determine the position and the orientation of the hydroxyl group. The so-called substitution structure (r_s) based on Kraitchman's equations,²² and the uncertainties from vibration-rotation effects as estimated by Costain⁴¹ ($\delta z = 0.0015/|z|$ Å) were used. The experimental positions of the hydroxyl hydrogen (OH) were obtained for all the four observed conformers. After a comparison between the obtained results of r_s coordinates of the hydroxyl group with those obtained theoretically at MP2 and B3LYP for the predicted conformers. The experimental coordinates of the hydrogen of OH match only the calculated values for Ia, IIa, IIIa, and IIIb conformers, their values are reported in Table III, the cartesian coordinates of all calculated conformers are reported in the SI. Thanks to the good agreement between the experimental and both theoretical results MP2 and B3LYP, the assignment of the four observed conformers is confirmed to be Ia, IIa, IIIa, and IIIb.

The relative abundances of the observed conformers can be estimated from the intensities of the rotational transitions, assuming that the adiabatic expansion brings all the molecules to the lowest vibrational state of each conformer. The relative population in our experiment follows the order $Ia \geq IIa > IIIa > IIIb$. These abundances are consistent with those obtained from the *ab initio* values at MP2/6-311++G(d,p) level of theory, and qualitatively consistent with the DFT values at B3LYP/6-311++G(d,p) by considering the Gibbs free energies calculated at 380 K.

Table III. Coordinates (a, b, c) in Å for the hydrogen atom of the OH group, for the four observed conformers of myrtenol compared to those obtained theoretically from MP2 and B3LYP methods with 6-311++G(d,p) basis set.

		a	b	c
Ia	Exp	$\pm 2.4962(6)$	$\pm 1.2444(12)$	$\pm 0.9726(15)$
	MP2	2.527	-1.179	1.001
	B3LYP	2.608	-1.255	1.000
IIa	Exp	$\pm 3.2243(5)$	$\pm 0.206(7)$	$\pm 1.0507(14)$
	MP2	3.205	-0.187	-1.040
	B3LYP	3.277	-0.218	-1.043
IIIa	Exp	$\pm 3.5975(4)$	$\pm 0.4257(35)$	$\pm 0.247(6)$
	MP2	3.548	0.496	-0.275
	B3LYP	3.614	0.475	-0.275
IIIb	Exp	$\pm 3.2430(6)$	$\pm 0.3516(52)$	$\pm 1.1061(17)$
	MP2	3.206	-0.322	1.117
	B3LYP	3.271	-0.378	1.122

The relaxed potential energy surface of myrtenol

An interesting fact, deduced from the present study, is the observation of only one conformer for I and II families (Ia and IIa) and two conformers for the family III (IIIa and IIIb). Furthermore, conformers IIIb and Ib having similar calculated energies, it is interesting to wonder why only IIIb conformer has been observed and why not Ib? Beside the small predicted dipole moment components of the Ib conformer, the non-observation of the conformer Ib could be attributed to an interconversion process as it has been observed before with other alcohols.^{14,42} The relaxation happens during the cooling process correlated with the supersonic expansion when the conformers are separated by low energy barriers (lower than $2kT$; where T is the temperature before the supersonic expansion).³⁵ This barrier is estimated to be about 530 cm^{-1} in our case. The relaxed potential energy surface (PES) of myrtenol has been explored along the $C_{\beta}-C_{\alpha}-O-H$ dihedral angle to determine the barrier height and explain any possible relaxation to the lowest energy conformers.

For the family I of conformers, the relaxed PES is shown in Figure 4. The barrier of interconversion is lower than 530 cm^{-1} , consequently, total or partial relaxation that can occur during the adiabatic expansion leads to the depopulation of both Ib and Ic conformers. The same fact is observed for the family II of conformers as shown in Figure 5. Again, conformers IIb and IIc may relax partially or totally to the more stable conformers. Therefore, the possible conformational relaxation could further decrease their population in the supersonic jet expansion **which**, together with their expected low abundance (high relative energies), leads to their non-observation in the supersonic expansion. On the contrary, for the family III of conformers, the

barrier of interconversion from IIIb to IIIa shown in Figure 6 is about two times higher (815 cm^{-1}), which is high enough to block the interconversion of the IIIb conformer. On the contrary, the IIIc conformer relaxes due to the small barrier separating it from the IIIa conformer.

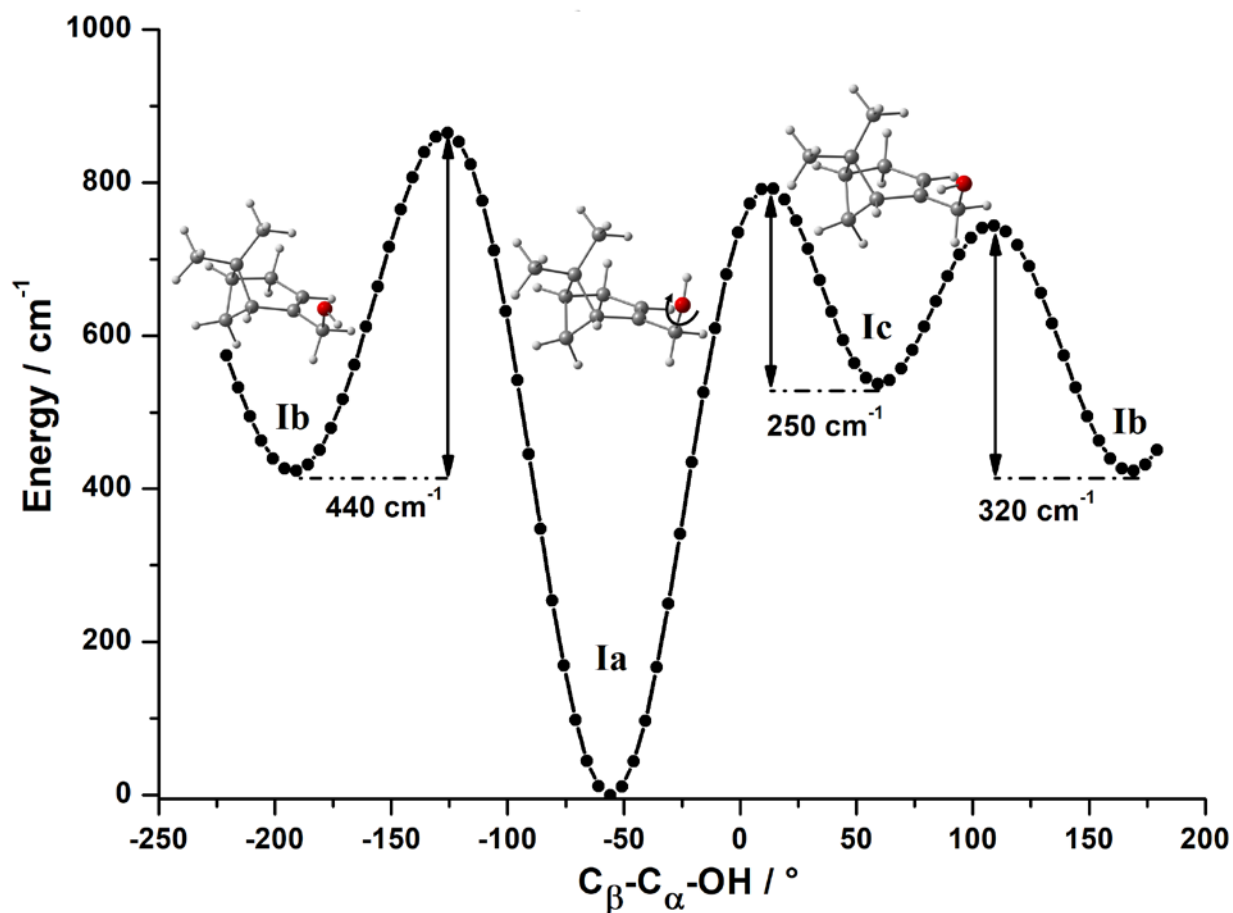


Figure 4. The relaxed potential energy surface of the hydroxyl functional group of myrtenol for the family I of conformers. The scan was made along the $C_{\beta}-C_{\alpha}-O-H$ dihedral angle as marked in the figure at the MP2/6-311++G(d,p) level of theory. As can be seen, the calculated barriers of interconversion are low ($\geq 450\text{ cm}^{-1}$).

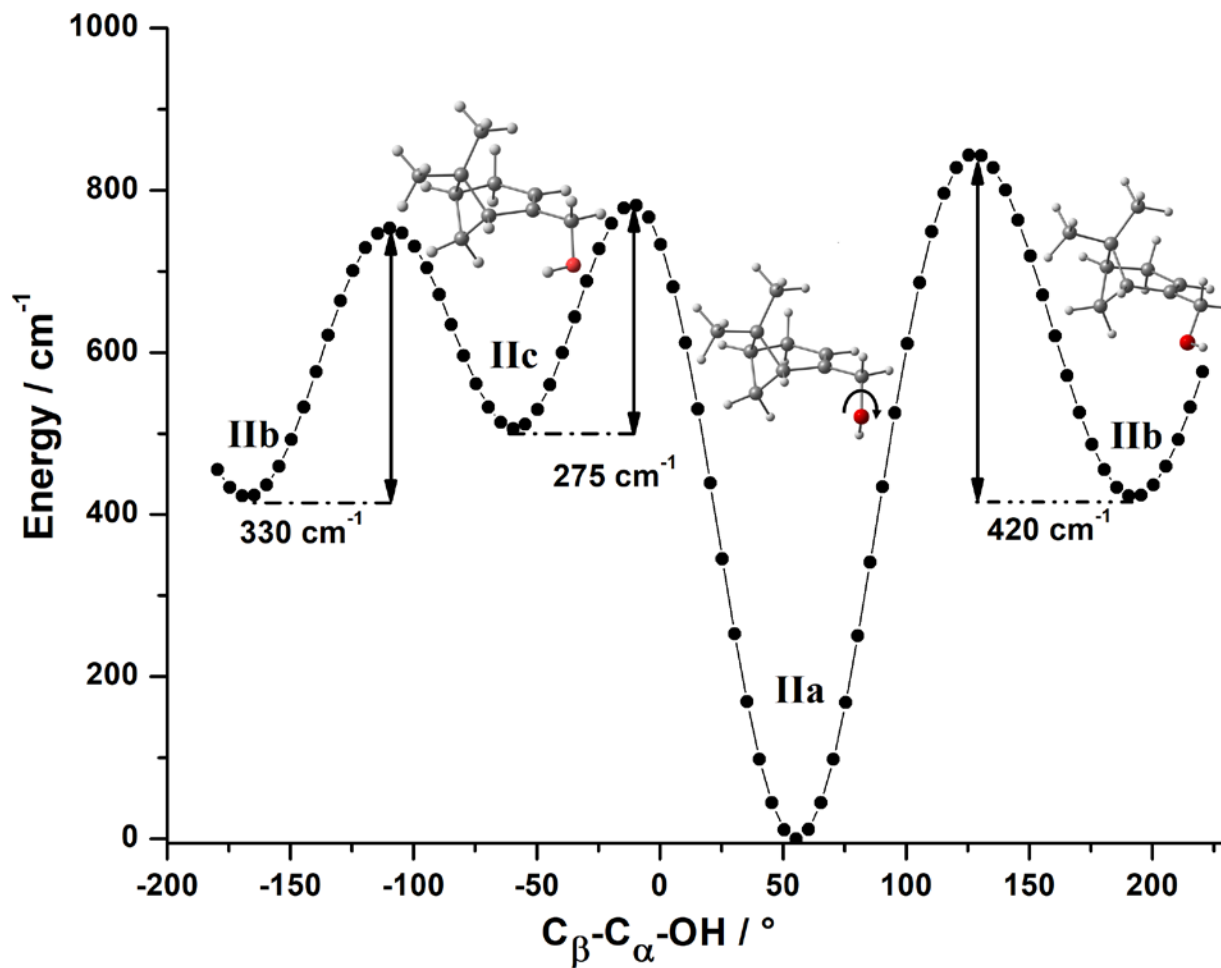


Figure 5. The relaxed potential energy surface of the hydroxyl functional group of myrtenol for the family II of conformers. The scan was made along the $\text{C}_\beta\text{-C}_\alpha\text{-O-H}$ dihedral angle as marked in the figure at the MP2/6-311++G(d,p) level of theory. As can be seen, the calculated barriers of interconversion are low ($\geq 450 \text{ cm}^{-1}$).

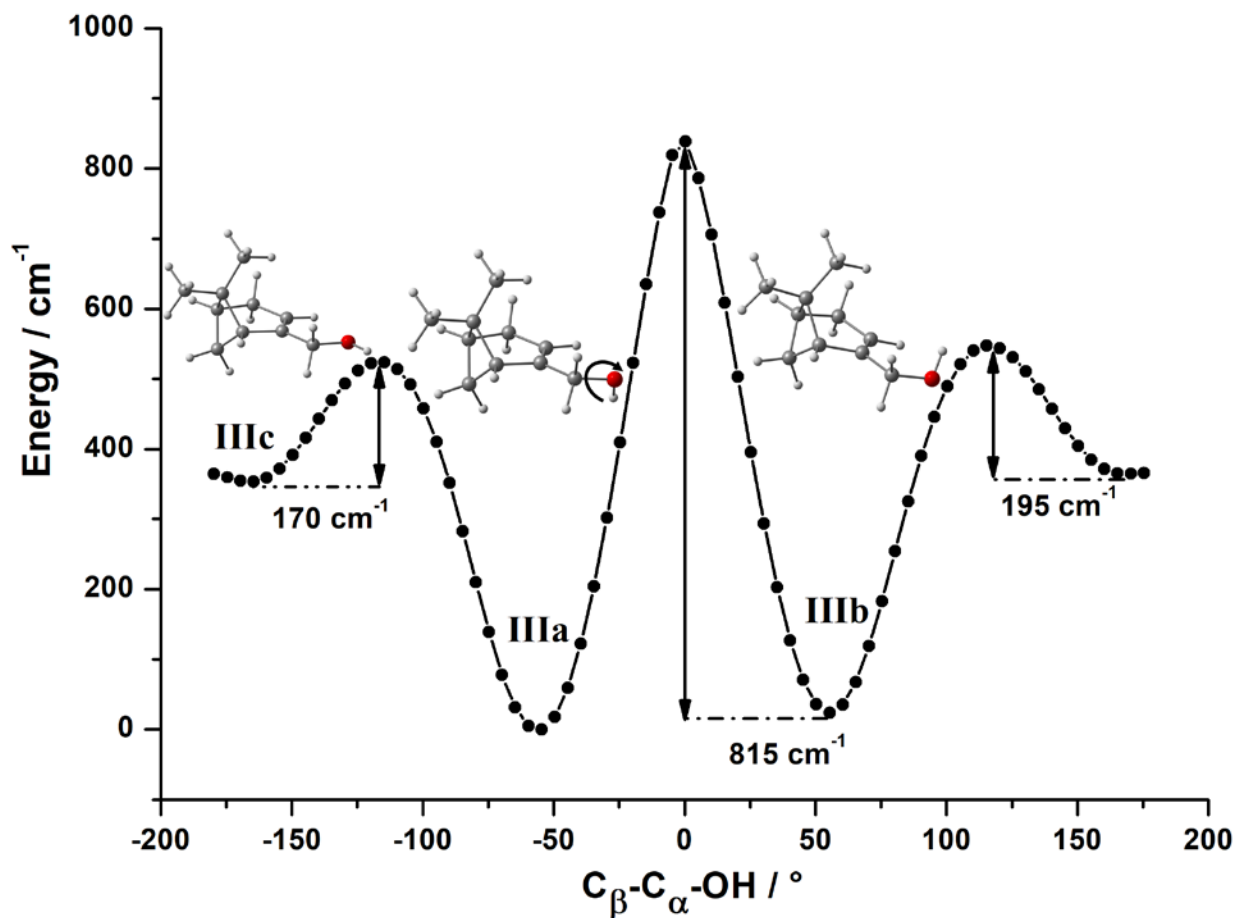


Figure 6. The relaxed potential energy surface of the hydroxyl functional group of myrtenol for the family III of conformers. The scan was made along the $C_{\beta}-C_{\alpha}-O-H$ dihedral angle as marked in the figure at the MP2/6-311++G(d,p) level of theory. As shown the calculated barrier of interconversion from conformer IIIb to IIIa is high enough (815 cm^{-1}) to prevent any relaxation of the IIIb conformer which leads to its experimental observation.

Finally, it should be noted that no relaxation between conformers is possible through the rotation of the $C_{\gamma}=C_{\beta}-C_{\alpha}-O$. Potential energy curves are presented in the supporting information (Figures S1, S2, S3). Indeed all barrier heights are higher than 760 cm^{-1} .

Comparison of allyl alcohol and myrtenol

Interestingly, the observed conformers of myrtenol adopt the same configuration as in allyl alcohol. This is illustrated with figure 7 and figure 8, which show a comparison between the iso-energetic structure of skew-gauche (ac, -sc) and syn-gauche (sp, sc) and the observed conformer of myrtenol Ia, IIa and IIIa, IIIb, respectively. Indeed the conformers Ia and IIa adopt the same structure skew-gauche (ac, -sc) as reported in the literature.^{19,20} In both conformers as in the skew-gauche (ac, -sc) a mirror structure could be observed. The structure parameters of both molecules are reported and compared in table IV. It is clear that the structure of the hydroxymethyl group in both allyl alcohol and myrtenol is quasi-conserved. The hydroxyl hydrogen is pointed towards the double bond π electronic system, suggesting stabilization energy due to the O-H $\cdots\pi$ internal hydrogen bond. This observation also explains the preference of those conformers and their stabilization. The structure of bonds and angles is quasi-unchanged between both molecules as could be observed in Table IV. However, a notable change is observed in the dihedral angles H-O-C-C and O-C-C=C values, of a few degrees. The explanation is that those angles are affected by the presence of the bicycle in myrtenol.

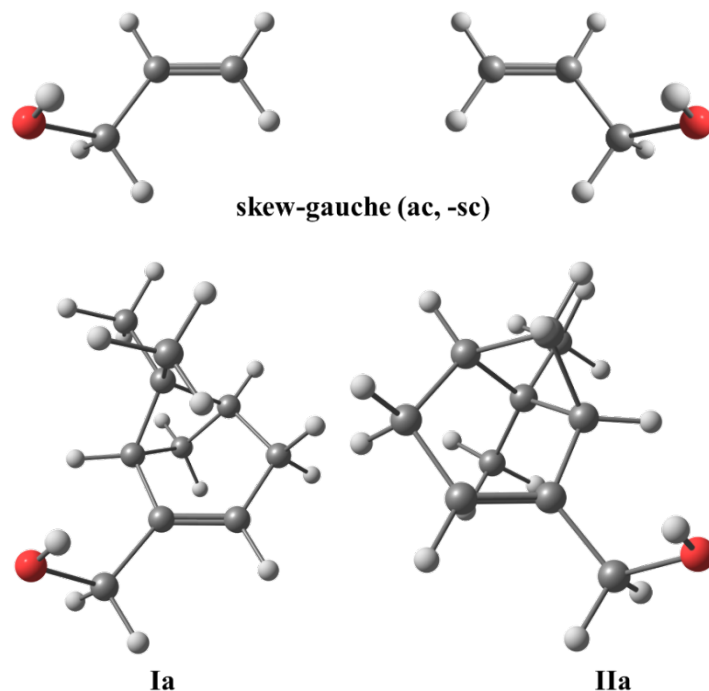


Figure 7. Structures of allyl alcohol skew-gauche (ac, -sc) and Ia and IIa of myrtenol. The views illustrate the similar structure of the hydroxymethyl functional group in both molecules

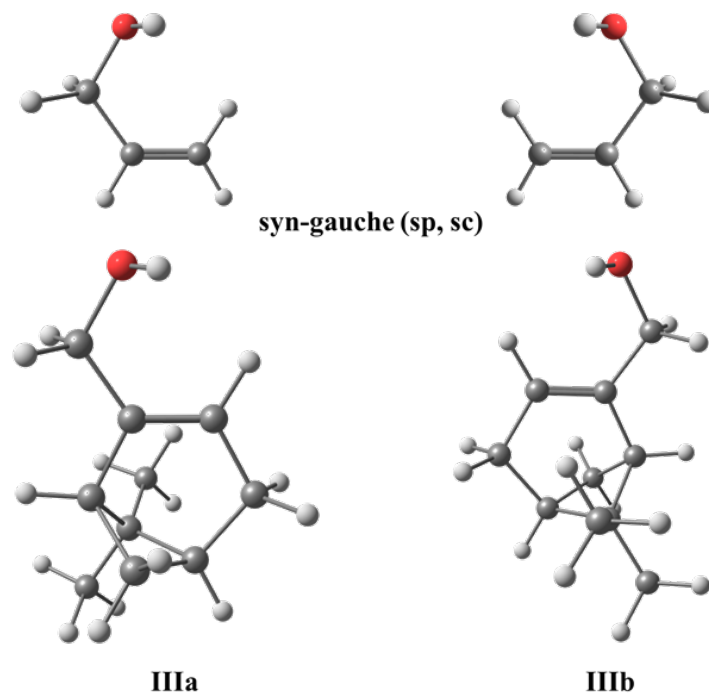


Figure 8. Structures of allyl alcohol syn-gauche (sp, sc) and of conformers IIIa and IIIb of myrtenol. The views illustrate the similar structure of the hydroxymethyl functional group in both molecules.

Table IV. Geometry comparison between the structure of allyl alcohol and myrtenol, at the MP2/6-311++G(d,p) level. Angles are given in degrees (°) and bonds in Å.

	Ia	(ac, -sc) ^a	IIa	(ac, -sc) ^a	IIIa	(sp, sc) ^b	IIIb	(sp, sc) ^b
O-H	0.963	0.961	0.963	0.961	0.962	0.962	0.962	0.962
O-C _α	1.433	1.429	1.432	1.429	1.418	1.418	1.418	1.418
C _α -C _β	1.498	1.500	1.498	1.500	1.504	1.505	1.504	1.505
C _β =C _γ	1.351	1.342	1.351	1.342	1.349	1.341	1.349	1.341
H-O-C _α	106.2	106.4	106.2	106.4	106.5	106.7	106.5	106.7
O-C _α -C _β	111.4	111.8	112.0	111.8	114.7	114.2	114.8	114.2
C _α -C _β =C _γ	123.2	123.2	123.2	123.2	124.9	124.7	125.0	124.7
H-O-C _α -C _β	-55.8	-54.4	55.4	54.4	-56.1	-58.1	55.4	58.1
O-C _α -C _β =C _γ	116.2	120.1	-119.3	-120.1	-5.3	-6.4	4.8	6.4

^a The two isoenergetic configurations of the (ac, -sc) conformer of allyl alcohol; ^b the two isoenergetic configurations of (sp, sc) conformer of allyl alcohol.

The myrtenol···water complex

The hydration of VOCs is relevant to understand the role of hydrogen bonding and its involvement in atmospheric chemistry at the molecular scale. A study investigating a hydrated monoterpene alcohol *endo* fenchol has been recently reported.¹⁵ A conformational change

associated with the hydroxyl group, and induced by the presence of one water molecule, has been observed. To check if any conformational change of OH is possible in the case of myrtenol, quantum chemical calculations were performed to explore the landscape of hydrated conformers for myrtenol. Five conformers were calculated below 700 cm^{-1} , their structures are reported in Figure 9. The most stable geometry Ia-1w(i) involves a proton donor ($\text{O}_w\text{-H}_w\cdots\text{O}$) water molecule. Interestingly, in the second most stable structure IIa-1w(i), water is acting as a proton acceptor, binding to the double bond of myrtenol and acting as a hydrogen bond donor by forming $\text{O}_w\text{-H}_w\cdots\pi$ bonds with a relative energy difference of only 288 cm^{-1} . The same bond type ($\text{O}_w\text{-H}_w\cdots\pi$) is observed in the highest energy conformers Ia-1w(ii) and IIIa-1w(i). As in the most stable conformer, a proton donor ($\text{O}_w\text{-H}_w\cdots\text{O}$) water molecule is observed also in the Ib-1w(i) conformer.

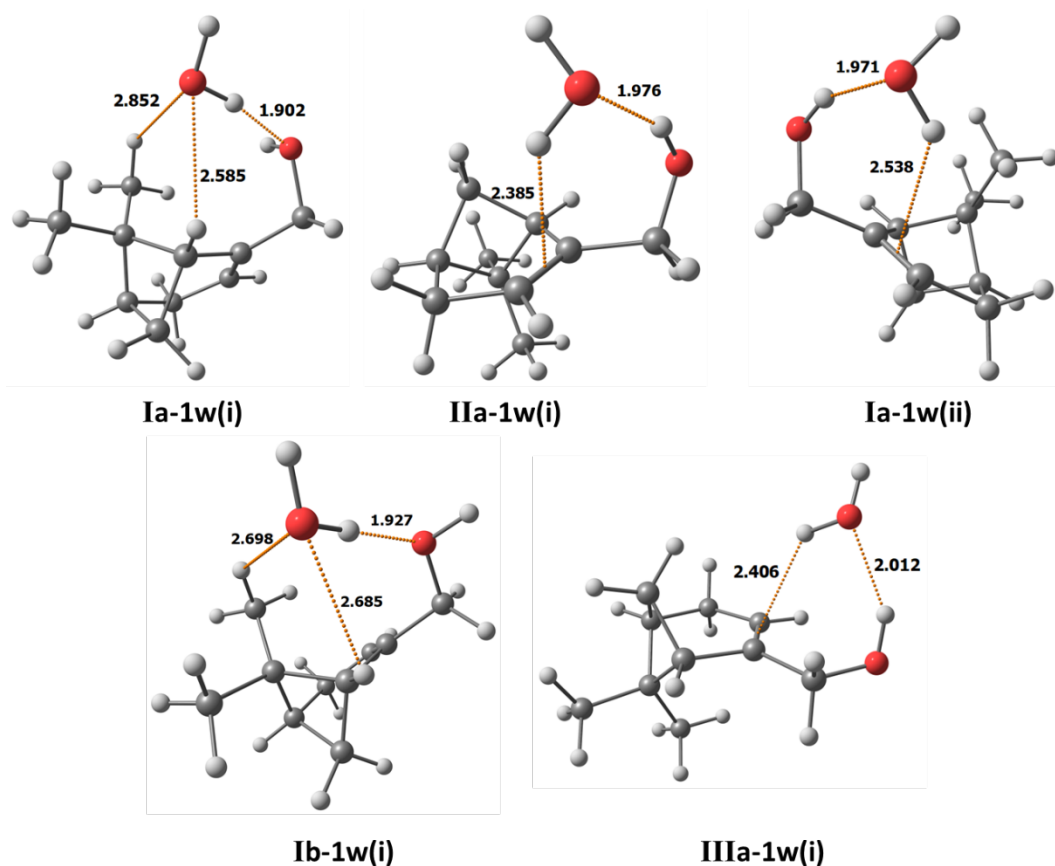


Figure 9. Equilibrium structures of the lowest energy conformers ($\leq 700 \text{ cm}^{-1}$) of the myrtenol...water complex calculated at MP2/6-311++G(d,p) level of theory. Bond lengths are given in Å.

Experimentally, pairs of b-type R-branch transitions were identified $(J+1)_{0,J+1} \leftarrow J_{1,J}$ and $(J+1)_{1,J+1} \leftarrow J_{0,J}$ (with $J=4,5,6$). Following iterative fittings and predictions, more b- and c-type transitions were measured and assigned. A total of 70 b-type and c-type transitions were recorded at high resolution (see examples of recorded transitions in figure 10) then fitted together with a Watson's Hamiltonian³⁸ in the S -reduction and I' representation. The obtained rotational parameters could match both conformers Ia-1w(i) and Ib-1w(i) since their values are slightly affected by the orientation of the hydrogen atoms of the water molecule or the hydroxyl group. As Ia-1w(i) is by far the lowest energy conformer, the observed species could be assigned

directly to it. The confirmation of the identity of the hydrated myrtenol conformer can be done by comparing the intensity of each type of observed transition with the calculated dipole moments. The intensity of the b-type and c-type transitions only matches the calculated dipole moment component of Ia-1w(i) conformer and not Ib-1w(i) conformer as no a-type transitions were observed in the spectra as shown in table IV. Another argument in favor of conformer Ia-1w(i) is that the experimental and calculated centrifugal distortion constant Δ_J match very well. Therefore, the identity of the observed conformer is confirmed unambiguously as Ia-1w(i). This observation confirms that no alteration of the hydroxyl group is induced by the presence of water. Additional trials and scans failed to identify other hydrated conformers in our supersonic jet.

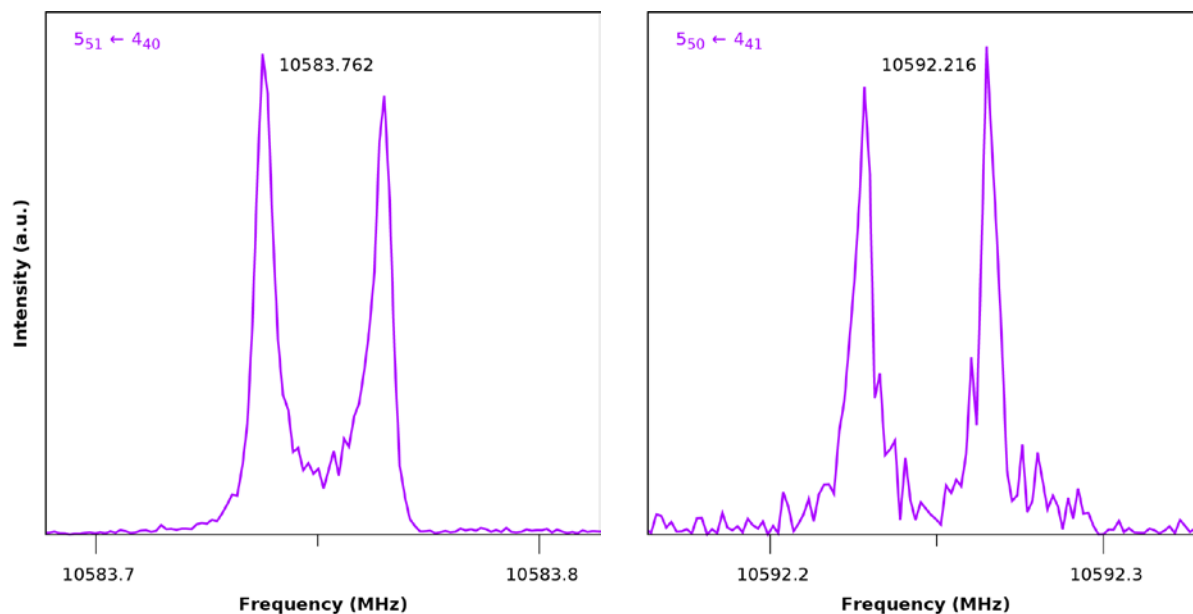


Figure 10. High-resolution transitions of the myrtenol···water complex (Ia-1w(i) conformer). All emission signals are split into Doppler doublets due to the collinear disposition between the supersonic jet expansion and the microwave resonator axis. The energy levels involved in each transition are labeled with the quantum numbers $J_{K_a K_c} \leftarrow J'_{K'_a K'_c}$.

Table V. Rotational constants, relative energies, and dipole moment components of the equilibrium structure of myrtenol...water conformers calculated at the MP2/6-311++G(d,p) level of theory.						
Constant ^a	Exp.	Ia-1w(i)	IIa-1w(i)	Ia-1w(ii)	Ib-1w(i)	IIIa-1w(i)
<i>A</i>	1094.851258(98)	1105.9	1392.9	1247.8	1085.4	1496.5
<i>B</i>	831.37506(39)	846.9	645.5	673.0	857.5	609.4
<i>C</i>	603.908210(73)	616.7	591.4	657.7	611.3	556.9
<i>D_J</i>	0.1561(19)	0.1284	0.0593	0.0716	0.0732	0.0450
<i>D_{JK}</i>	-0.0549(28)	-0.0343	-0.1315	0.0767	0.1758	-0.0591
<i>D_K</i>	-	-0.0018	0.3430	0.0221	-0.1682	0.2263
<i>d₁</i>	-0.0519(13)	-0.0438	-0.0032	-0.0055	-0.0226	-0.0030
<i>d₂</i>	-0.00387(43)	-0.00366	0.00036	-0.00161	-0.00571	0.00014
<i>rms</i> ^b	1.9	-	-	-	-	-
<i>N</i> ^c	70	-	-	-	-	-
<i>κ</i> ^d	-0.07	-0.06	-0.87	-0.95	0.04	-0.89
<i>μ_a</i>	Not observed	0.2	1.7	1.6	1.4	1.4
<i>μ_b</i>	Observed	1.7	2.9	0.9	2.4	2.8
<i>μ_c</i>	Observed	0.8	0.1	2.6	0.2	0
<i>ΔE</i> ^e		0	284	535	630	665

^a *A*, *B*, and *C* are the rotational constants given in MHz; *D_J*, *D_{JK}*, *D_K*, *d₁*, and *d₂* are the quartic centrifugal distortion constant given in kHz; absolute values of *μ_a*, *μ_b*, and *μ_c* represent the electric dipole moment components in D (1 D ≈ 3.3356×10⁻³⁰ C m). ^b standard deviation of the fit in kHz. ^c number of fitted lines. ^d $\kappa = (2B - A - C)/(A - C)$; ^e *ΔE* are the relative electronic energies in cm⁻¹ with respect to the global minima calculated at the MP2/6-311++G(d,p) level.

The importance of the dispersion interaction in the stabilization of the highest energy conformer upon hydration, responsible for the conformational change, has been recently reported in the

case of *endo* fenchol.¹⁵ To map these interactions in the case of myrtenol, a Non-Covalent Interaction (NCI) analysis³⁵ of the electron density and its derivative has been performed using the Multiwfn software³⁶ using the MP2/6-311++G(d,p) level of theory output. This analysis shows (see figure 11) a blue iso-surface representing a strong hydrogen bond ($\text{HOH}_{\text{water}} \cdots \text{OH}$) linking water to the OH-myrtenol (conformer Ia). The green iso-surface indicates three weak interactions $\text{CH} \cdots \text{O}_{\text{water}}$. The weak dispersive interactions play an important role in the stabilization of this conformer.

The stability of the lowest energy conformer of the myrtenol \cdots water complex can be attributed to the strong inter-molecular and dispersive interactions. Natural bond orbital (NBO) analysis³⁴ was performed at the MP2/6-311++G(d,p) level for the Ia-1w(i) conformer. It provides an intuitive framework to rationalize the transfer of electronic charges associated with those interactions. The values obtained from the NBO analysis reflect an appreciable degree of charge delocalization in the intermolecular Hydrogen bond that stabilizes the structure by the intermolecular interactions between lone pair (LP) of myrtenol oxygen and anti-bonding orbitals (BD*) of O-H of water molecules. This dominant interaction occurs between n orbital of $\text{O}_{\text{myrtenol}}$ and BD* orbital of $\text{O}_w\text{-H}_w$ with stabilization energies of 10 and 30 $\text{kJ}\cdot\text{mol}^{-1}$. The dispersive stabilization energies between O_{water} and the three hydrogens of myrtenol $\text{H}_{\text{myrtenol}}$ are calculated to be 0.7 and 1.3 $\text{kJ}\cdot\text{mol}^{-1}$.

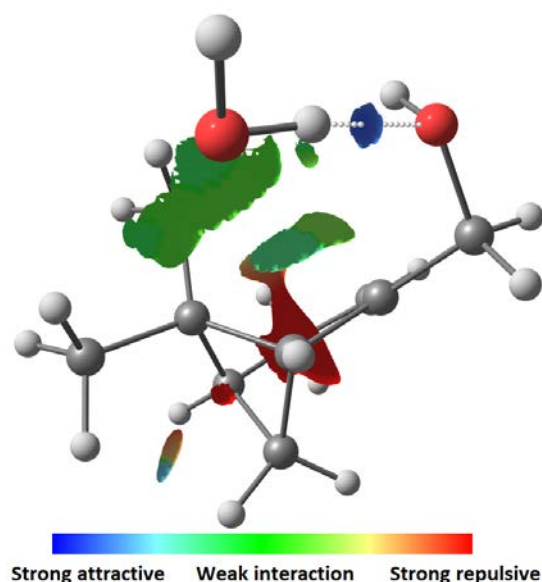


Figure 11. NCI plots showing the interactions involved in the stabilization of the observed structure Ia-1w(i) of myrtenol...water.

Conclusion

The conformational behavior of myrtenol and its weakly bound 1:1 complex with water was investigated using a synergic combination of Fourier transform microwave spectroscopy and theoretical calculations. Under isolated conditions, four conformers of myrtenol with different orientations of the hydroxymethyl group have been observed, characterized, and identified. The position of the hydroxyl group was evidenced for each conformer by its deuteration, which allows the determination of the substitution structure. For the I and II families, only one conformer (Ia and IIa) has been observed among the three calculated structures. The non-observation of the other conformers is attributed to the conformational relaxation process that takes place in supersonic jet expansion due to the small barrier height of interconversion that separates the conformers. On the contrary, the high barrier height of interconversion found in the III family,

and prevents the relaxation, leading to the observation of the two conformers IIIa and IIIb. The good agreement between experimental and theoretical studies is an indication that the characterization of bicyclic alcohol structures with accuracy is becoming possible. Furthermore, the hydration of myrtenol has been also studied. The lowest energy conformer myrtenol...water has been identified. It is the most stable conformer of myrtenol forming a hydrogen bond with water (Ia-1w(i)). The formation of the hydrogen bond between myrtenol and water acting as a proton donor does not alter the arrangement of the hydroxyl group. Our study shows the robustness of the structure of the hydroxymethyl group upon hydration by conserving the same structure as in the allyl alcohol. This study could be interesting for atmospheric chemistry helping us to understand the process of atmospheric aerosol formation.

Conflicts of interest

There are no conflicts to declare.

Acknowledgments

The present work was funded by the French ANR *Labex CaPPA* through the PIA under contract ANR-11-LABX-0005-01, by the Regional Council *Hauts-de-France*, and by the European Funds for Regional Economic Development (FEDER). It is a contribution to the scientific project CPER CLIMIBIO. E. M. N. would like to thank the CNRS for a researcher contract.

References

¹ D. Kotzias, J.L. Hjorth, and H. Skov, *Toxicol. Environ. Chem.* **20–21**, 95 (1989).

- ² T. Hoffmann, J.R. Odum, F. Bowman, D. Collins, D. Klockow, R.C. Flagan, and J.H. Seinfeld, *J. Atmos. Chem.* **26**, 189 (1997).
- ³ A.B. Guenther, X. Jiang, C.L. Heald, T. Sakulyanontvittaya, T. Duhl, L.K. Emmons, and X. Wang, *Geosci. Model Dev.* **5**, 1471 (2012).
- ⁴ J.-F. Müller, T. Stavrakou, S. Wallens, I. De Smedt, M. Van Roozendaal, M.J. Potosnak, J. Rinne, B. Munger, A. Goldstein, and A.B. Guenther, *Atmos. Chem. Phys.* **8**, 1329 (2008).
- ⁵ J.H. Kroll and J.H. Seinfeld, *Atmos. Environ.* **42**, 3593 (2008).
- ⁶ S. Fuzzi, U. Baltensperger, K. Carslaw, S. Decesari, H. Denier Van Der Gon, M.C. Facchini, D. Fowler, I. Koren, B. Langford, U. Lohmann, E. Nemitz, S. Pandis, I. Riipinen, Y. Rudich, M. Schaap, J.G. Slowik, D. V Spracklen, E. Vignati, M. Wild, M. Williams, and S. Gilardoni, *Atmos. Chem. Phys.* **15**, 8217 (2015).
- ⁷ I. Manisalidis, E. Stavropoulou, A. Stavropoulos, and E. Bezirtzoglou, *Front. Public Heal.* **8**, 14 (2020).
- ⁸ E.M. Neeman, J.R. Avilés Moreno, and T.R. Huet, *J. Chem. Phys.* **147**, 214305 (2017).
- ⁹ E.M. Neeman, J.R. Avilés-Moreno, and T.R. Huet, *Phys. Chem. Chem. Phys.* **19**, 13819 (2017).
- ¹⁰ C. Pio, C. Alves, and A. Duarte, *Atmos. Environ.* **35**, 389 (2001).
- ¹¹ C.A. Pio, C.A. Alves, and A.C. Duarte, *Atmos. Environ.* **35**, 1365 (2001).
- ¹² G. Flamini and P.L. Cioni, *Food Chem.* **120**, 984 (2010).
- ¹³ L.T. Huong, N.T. Thuong, L.D. Chac, D.N. Dai, A.O. Giwa-Ajeniya, and I.A. Ogunwande, *Am. J. Essent. Oils Nat. Prod.* **8**, 09 (2020).
- ¹⁴ E.M. Neeman and T.R. Huet, *Phys. Chem. Chem. Phys.* **20**, 24708 (2018).
- ¹⁵ E.M. Neeman and T.R. Huet, *Phys. Chem. Chem. Phys.* **23**, 2179 (2021).
- ¹⁶ L. Evangelisti, Q. Gou, G. Feng, W. Caminati, G.J. Mead, I.A. Finneran, P.B. Carroll, and G.A. Blake, *Phys. Chem. Chem. Phys.* **19**, 568 (2017).
- ¹⁷ E.M. Neeman, J.R. Aviles Moreno, and T.R. Huet, *Phys. Chem. Chem. Phys.* **23**, 18137 (2021).
- ¹⁸ G. Sedo, F.E. Marshall, and G.S. Grubbs, *J. Mol. Spectrosc.* **356**, 32 (2019).
- ¹⁹ S. Melandri, P.G. Favero, and W. Caminati, *Chem. Phys. Lett.* **223**, 541 (1994).
- ²⁰ F. Vanhouteghem, W. Pyckhout, C. Van Alsenoy, L. Van Den Enden, and H.J. Geise, *J. Mol. Struct.* **140**, 33 (1986).
- ²¹ M. Tudorie, L.H. Coudert, T.R. Huet, D. Jegouso, and G. Sedes, *J. Chem. Phys.* **134**, 074314 (2011).
- ²² J. Kraitchman, *Am. J. Phys.* **21**, 17 (1953).

- ²³ A. Laaksonen, J. Malila, and A. Nenes, *Atmos. Chem. Phys.* **20**, 13579 (2020).
- ²⁴ D.R. Cocker, S.L. Clegg, R.C. Flagan, and J.H. Seinfeld, *Atmos. Environ.* **35**, 6049 (2001).
- ²⁵ C.J. Hennigan, M.H. Bergin, and R.J. Weber, *Environ. Sci. Technol.* **42**, 9079 (2008).
- ²⁶ C.J. Hennigan, M.H. Bergin, J.E. Dibb, and R.J. Weber, *Geophys. Res. Lett.* **35**, L18801 (2008).
- ²⁷ R. Zhang, *Science* **328**, 1366 (2010).
- ²⁸ M. Kulmala, L. Pirjola, and J.M. Mäkelä, *Nature* **404**, 66 (2000).
- ²⁹ M.J. Frisch, G.W. Trucks, H.B. Schlegel, G.E. Scuseria, M.A. Robb, J.R. Cheeseman, G. Scalmani, V. Barone, G.A. Petersson, H. Nakatsuji, X. Li, M. Caricato, A. V. Marenich, J. Bloino, B.G. Janesko, R. Gomperts, B. Mennucci, H.P. Hratchian, J. V. Ortiz, A.F. Izmaylov, J.L. Sonnenberg, D. Williams-Young, F. Ding, F. Lipparini, F. Egidi, J. Goings, B. Peng, A. Petrone, T. Henderson, D. Ranasinghe, V.G. Zakrzewski, J. Gao, N. Rega, G. Zheng, W. Liang, M. Hada, M. Ehara, K. Toyota, R. Fukuda, J. Hasegawa, M. Ishida, T. Nakajima, Y. Honda, O. Kitao, H. Nakai, T. Vreven, K. Throssell, J.A. Montgomery, Jr., J.E. Peralta, F. Ogliaro, M.J. Bearpark, J.J. Heyd, E.N. Brothers, K.N. Kudin, V.N. Staroverov, T.A. Keith, R. Kobayashi, J. Normand, K. Raghavachari, A.P. Rendell, J.C. Burant, S.S. Iyengar, J. Tomasi, M. Cossi, J.M. Millam, M. Klene, C. Adamo, R. Cammi, J.W. Ochterski, R.L. Martin, K. Morokuma, O. Farkas, J.B. Foresman, and D.J. Fox, *Gaussian 16*, Rev. C. 01 Gaussian Inc. (2016).
- ³⁰ C. Møller and M.S. Plesset, *Phys. Rev.* **46**, 618 (1934).
- ³¹ C. Lee, W. Yang, and R.G. Parr, *Phys. Rev. B* **37**, 785 (1988).
- ³² A.D. Becke, *J. Chem. Phys.* **98**, 5648 (1993).
- ³³ L.A. Curtiss, K. Raghavachari, P.C. Redfern, V. Rassolov, and J.A. Pople, *J. Chem. Phys.* **109**, 7764 (1998).
- ³⁴ J.P. Foster and F. Weinhold, *J. Am. Chem. Soc.* **102**, 7211 (1980).
- ³⁵ E.R. Johnson, S. Keinan, P. Mori-Sánchez, J. Contreras-García, A.J. Cohen, and W. Yang, *J. Am. Chem. Soc.* **132**, 6498 (2010).
- ³⁶ T. Lu and F. Chen, *J. Comput. Chem.* **33**, 580 (2012).
- ³⁷ S. Kassi, D. Petitprez, and G. Wlodarczak, *J. Mol. Struct.* **517**, 375 (2000).
- ³⁸ J.K.G. Watson, in *Vib. Spectra Struct. Vol.6. A Ser. Adv.* (1977), pp. 1–89.
- ³⁹ H.M. Pickett, *J. Mol. Spectrosc.* **148**, 371 (1991).
- ⁴⁰ Z. Kisiel, *In Spectroscopy from Space, Ed. J. Demaison, et Al., Kluwer Academic Publishers, Dordrecht, 2001, Pp. 91–106; PROSPE – Programs for ROTational SPECTroscopy, Institute of Physics, Academy of Science, Warsaw, [Http://Www.Ifpan.Edu.Pl/~kisiel/Prospe.Htm](http://Www.Ifpan.Edu.Pl/~kisiel/Prospe.Htm) (n.d.)*
- ⁴¹ C.C. Costain, *Trans. Am. Cryst. Assoc.* **2**, 157 (1966).

⁴² R.S. Ruoff, T.D. Klots, T. Emilsson, and H.S. Gutowsky, *J. Chem. Phys.* **93**, 3142 (1990).